AMERICAN SOCIETY FOR MICROBIOLOGY | Journal of Virology

A Library of Infectious Hepatitis C Viruses with Engineered Mutations in the E2 Gene Reveals Growth-Adaptive Mutations That Modulate Interactions with Scavenger Receptor Class B Type I

Adam Zuiani,[a] Kevin Chen,[b] Megan C. Schwarz,[f] James P. White,[c] Vincent C. Luca,[g] Daved H. Fremont,[a,b,d] David Wang,[a,b] Matthew J. Evans,[f] Michael S. Diamond[a,b,c,e]

Departments of Pathology and Immunology,[a] Molecular Microbiology,[b] Medicine,[c] and Biochemistry and Molecular Biophysics[d] and the Center for Human Immunology and Immunotherapy Programs,[e] Washington University School of Medicine, St. Louis, Missouri, USA; Department of Microbiology, Icahn School of Medicine at Mount Sinai, New York, New York, USA[f]; Departments of Molecular and Cellular Physiology and Structural Biology and the Howard Hughes Medical Institute, Stanford University School of Medicine, Stanford, California, USA[g]

ABSTRACT

While natural hepatitis C virus (HCV) infection results in highly diverse quasispecies of related viruses over time, mutations accumulate more slowly in tissue culture, in part because of the inefficiency of replication in cells. To create a highly diverse population of HCV particles in cell culture and identify novel growth-enhancing mutations, we engineered a library of infectious HCV with all codons represented at most positions in the ectodomain of the E2 gene. We identified many putative growth-adaptive mutations and selected nine highly represented E2 mutants for further study: Q412R, T416R, S449P, T563V, A579R, L619T, V626S, K632T, and L644I. We evaluated these mutants for changes in particle-to-infectious-unit ratio, sensitivity to neutralizing antibody or CD81 large extracellular loop (CD81-LEL) inhibition, entry factor usage, and buoyant density profiles. Q412R, T416R, S449P, T563V, and L619T were neutralized more efficiently by anti-E2 antibodies and T416R, T563V, and L619T by CD81-LEL. Remarkably, all nine variants showed reduced dependence on scavenger receptor class B type I (SR-BI) for infection. This shift from SR-BI usage did not correlate with a change in the buoyant density profiles of the variants, suggesting an altered E2-SR-BI interaction rather than changes in the virus-associated lipoprotein-E2 interaction. Our results demonstrate that residues influencing SR-BI usage are distributed across E2 and support the development of large-scale mutagenesis studies to identify viral variants with unique functional properties.

IMPORTANCE

Characterizing variant viruses can reveal new information about the life cycle of HCV and the roles played by different viral genes. However, it is difficult to recapitulate high levels of diversity in the laboratory because of limitations in the HCV culture system. To overcome this limitation, we engineered a library of mutations into the E2 gene in the context of an infectious clone of the virus. We used this library of viruses to identify nine mutations that enhance the growth rate of HCV. These growth-enhancing mutations reduced the dependence on a key entry receptor, SR-BI. By generating a highly diverse library of infectious HCV, we mapped regions of the E2 protein that influence a key virus-host interaction and provide proof of principle for the generation of large-scale mutant libraries for the study of pathogens with great sequence variability.

Hepatitis C virus (HCV) infection causes a major global health burden, as approximately 3% of the world's population is affected (1). Up to 30% of individuals with HCV will resolve infection spontaneously, whereas the majority develop chronic infections that can cause fibrosis, cirrhosis, and hepatocellular carcinoma (2). HCV is a member of the hepacivirus genus of the *Flaviviridae* family of RNA viruses and is a positive-sense, enveloped virus with a 9.6-kb genome. The genome comprises a single open reading frame encoding an approximately 3,000-amino-acid polyprotein flanked by 5′- and 3′-noncoding regions. HCV primarily infects and replicates in hepatocytes, and its life cycle is tied intimately to the lipoprotein biosynthesis pathway. HCV particles incorporate host lipoproteins, forming a "lipoviroparticle" with unique properties compared to other *Flaviviridae* members (3, 4).

HCV is divided into 7 genotypes and 67 subtypes and exists as a quasispecies within a host (5). Natural HCV isolates exhibit considerable diversity in their genomic sequences; however, it is difficult to recapitulate the extent of this variability *in vitro*. Recent advances have made it possible to infect cells in culture with human-derived HCV isolates and observe genome replication, but new infectious particles still cannot be generated readily from clinical samples (6). The study of cell culture infectious HCV relies on a few relatively slow-growing infectious clones (7–13). These clones do not acquire growth-adaptive mutations rapidly during passaging despite the high error rate of the HCV polymerase, possibly because of the limited production of new infectious virions.

HCV has two envelope glycoproteins, E1 and E2. The product

Received 23 May 2016 **Accepted** 7 September 2016

Accepted manuscript posted online 14 September 2016

Citation Zuiani A, Chen K, Schwarz MC, White JP, Luca VC, Fremont DH, Wang D, Evans MJ, Diamond MS. 2016. A library of infectious hepatitis C viruses with engineered mutations in the E2 gene reveals growth-adaptive mutations that modulate interactions with scavenger receptor class B type I. J Virol 90: 10499–10512. doi:10.1128/JVI.01011-16.

Editor: J.-H. J. Ou, University of Southern California

Address correspondence to Michael S. Diamond, diamond@borcim.wustl.edu.

of the E2 gene is a protein of particular variability and is under selection pressure from adaptive immune responses during an extended chronic infection (14, 15). In conjunction with virus-associated lipoprotein, the envelope proteins mediate attachment and entry of the virus into host cells (16). E1 and E2 form noncovalently linked trimers of disulfide-linked heterodimers on the virion surface (17, 18). Two partial crystal structures of the core of the E2 protein have provided some insight into E2 structural biology (19, 20). E2 core has a compact, globular structure consisting mainly of random coils and β-strands. While several structural features of E2 have well-described functions in the HCV life cycle, the contributions of other regions of the protein are less well understood (21–24).

To study an HCV population containing an array of single-amino-acid variants, we created a genotype 2a JFH-1 isolate library with maximal diversity in the E2 gene. We generated a site-directed saturation mutagenesis (SDSM) library from a JFH-1-derived infectious clone, which allowed us to explore almost the entire sequence space for single-codon substitutions in E2. We used the library to identify novel E2 growth-adaptive mutations. After only three passages, nine mutations in different regions of the protein were identified and confirmed to have growth kinetic advantages: Q412R, T416R, S449P, T563V, A579R, L619T, V626S, K632T, and L644I. These mutants had various profiles with respect to neutralizing monoclonal antibody (NMAb) and CD81 large extracellular loop (CD81-LEL) sensitivity. However, all of these mutations yielded a reduced dependence on scavenger receptor class B type I (SR-BI) for entry, even though they were distributed across several regions of E2. Our study provides insight into the molecular determinants of the interaction between SR-BI and E2 and acts as proof of principle for the use of large-scale variant libraries to address questions in HCV biology.

MATERIALS AND METHODS

Cell culture. Huh7.5 cells were obtained as a gift (C. Rice, Rockefeller University) and maintained in Dulbecco's modified Eagle medium (DMEM; Thermo Fisher Scientific) supplemented with 10% fetal bovine serum (FBS; Equitech-Bio), MEM nonessential amino acids, and penicillin-streptomycin (Corning).

Plasmid library and virus production. The plasmid pLJ83, which encodes the JFH-1 HCV infectious clone bearing adaptive mutations outside the E2 gene, was a generous gift (G. Luo, University of Alabama, Birmingham) (25) and was used for our SDSM library. Unless noted in the text, all amino acid residue numbers refer to the JFH-1 genome (26). Three hundred twenty complementary primer sets containing random nucleotides at all three positions of a single codon within the E2 gene were designed and ordered from Integrated DNA Technologies. All residues between amino acid positions 384 and 721 in the polyprotein were targeted, excluding cysteines (positions 429, 452, 459, 488, 496, 505, 510, 554, 566, 571, 585, 589, 601, 611, 624, 648, 656, and 681). Each primer set was used to amplify variants by PCR from pLJ83 using a Phusion high-fidelity polymerase kit (New England BioLabs). The PCR products were digested with DpnI (New England BioLabs) and transformed in library-grade MegaX DH10B T1R electrocompetent cells (Thermo Fisher Scientific).

Plasmids were prepared from bacterial cultures using plasmid Maxiprep kits (Qiagen) from sets of 10 sequential codon libraries generated by SDSM. The 32 pooled plasmid libraries corresponded to the following amino acids: 384 to 393, 394 to 403, 404 to 413, 414 to 423, 424 to 434, 435 to 444, 445 to 455, 456 to 466, 467 to 476, 477 to 486, 487 to 498, 499 to 509, 511 to 520, 521 to 530, 531 to 540, 541 to 550, 551 to 561, 562 to 573, 574 to 583, 584 to 595, 596 to 606, 607 to 617, 618 to 628, 629 to 638, 639 to 649, 650 to 660, 661 to 670, 671 to 680, 682 to 691, 692 to 701, 702 to 711, and 712 to 721. The plasmids were linearized by digestion with NruI (New England BioLabs) and purified, and genomic RNA was synthesized using a MEGAscript T7 transcription kit (Ambion). Infectious HCV was generated after transfection of Huh7.5 cells by electroporating 2 μg of *in vitro*-derived viral RNA into 4×10^6 Huh7.5 cells, and virus was harvested 48, 72, 96, and 120 h later. HEPES, pH 7.3 (10 mM), was added to the virus-containing supernatants for storage at 4°C prior to concentration with Amicon Ultra 100,000-kDa-molecular-size-cutoff centrifugal filters (EMD Millipore). Concentrated virus stocks were stored at −80°C, and titers were determined using the 50% tissue culture infectious dose ($TCID_{50}$) method (27).

Amplicon sequencing of plasmid libraries. The 32 sets of pooled plasmids described above were analyzed using next-generation sequencing to determine the diversity of the library. An approximately 2-kb fragment corresponding to the E1 and E2 genes was amplified by PCR from each of the 32 plasmid pools and submitted for Ampicon-Seq library preparation and Illumina HiSeq sequencing (single-end 50-bp reads) at the Genome Technology Access Center at Washington University. Reads were aligned to the pLJ83 sequence using Bowtie2. Reads containing an insertion or deletions were not considered, and the remaining reads were counted to determine codon frequency using a custom script.

FFA. Infectious HCV was detected using a focus-forming assay (FFA) on Huh7.5 cells. Briefly, 6.4×10^3 Huh7.5 cells were plated in individual wells of a 96-well plate treated with poly-L-lysine 1 day prior to infection. Three days later, cells were rinsed with phosphate-buffered saline (PBS), fixed, permeabilized with cold methanol, rinsed again, and incubated in blocking solution (PBS containing 1% bovine serum albumin [BSA] and 0.2% skim milk). Subsequently, the cells were incubated with 100 ng/ml anti-NS5A MAb (9E10; a gift of C. Rice, Rockefeller University [9]), rinsed again, and incubated with a 1:2,000 dilution of horseradish peroxidase-conjugated goat anti-mouse IgG (Sigma). Virus-infected cell foci were visualized using TrueBlue peroxidase reagent (KPL) and quantified using an S5 BioSpot Macroanalyzer (Cellular Technologies Ltd.).

Selection of mutations in E2 that confer increased HCV growth. Parallel cultures of 3.8×10^4 Huh7.5 cells were infected with 1×10^4 $TCID_{50}$ of each of 32 HCV mutant pools containing engineered diversity at 10 sequential positions in E2. Input viruses were removed 6 h postinfection, and newly generated viruses were harvested 7 days later and used to infect new Huh7.5 cells. This process was performed twice for a total of three passages. After the third passage, viral RNA was harvested using QIAamp viral RNA minikits (Qiagen) from all 32 final-passage viruses, cDNAs were synthesized using the Superscript III first-strand synthesis system (Invitrogen), and DNA fragments corresponding to the E1-E2 fragment were amplified by PCR. Each PCR product was sequenced across the region of the E2 gene containing the sites of engineered mutations in the original pool. If changes to the consensus sequence were observed, the exact combinations of nucleotide substitutions at any given codon were determined using a Zero Blunt TOPO PCR cloning kit (Invitrogen) to generate individual bacterial colonies bearing unique E1-E2 sequences. Nine mutations identified from the TOPO cloning results were introduced into pLJ83 using conventional site-directed mutagenesis. Following verification of the complete genome sequence of the mutant plasmids, all nine clonal mutant viruses were generated as described above. Three of the nine selected mutations (S449P, L619T, and L644I) also were introduced into a JFH-1-derived chimeric infectious clone encoding the structural genes of the genotype 1 H77 isolate (H77/JFH-1) at homologous positions in the E2 gene (28). The corresponding mutations in the H77 strain were S449P, L615T, and L640I. Virus was produced exactly as described above, except XbaI instead of NruI restriction enzyme digestion was performed prior to *in vitro* RNA production.

Alignment of genotype 2 E2 amino acid sequences. To determine if the substitutions selected were present in circulating HCV strains, an alignment of genotype 2 E2 sequences was generated using the NIAID Virus Pathogen Database and Analysis Resource (ViPR) (http://www.viprbrc.org/) (29).

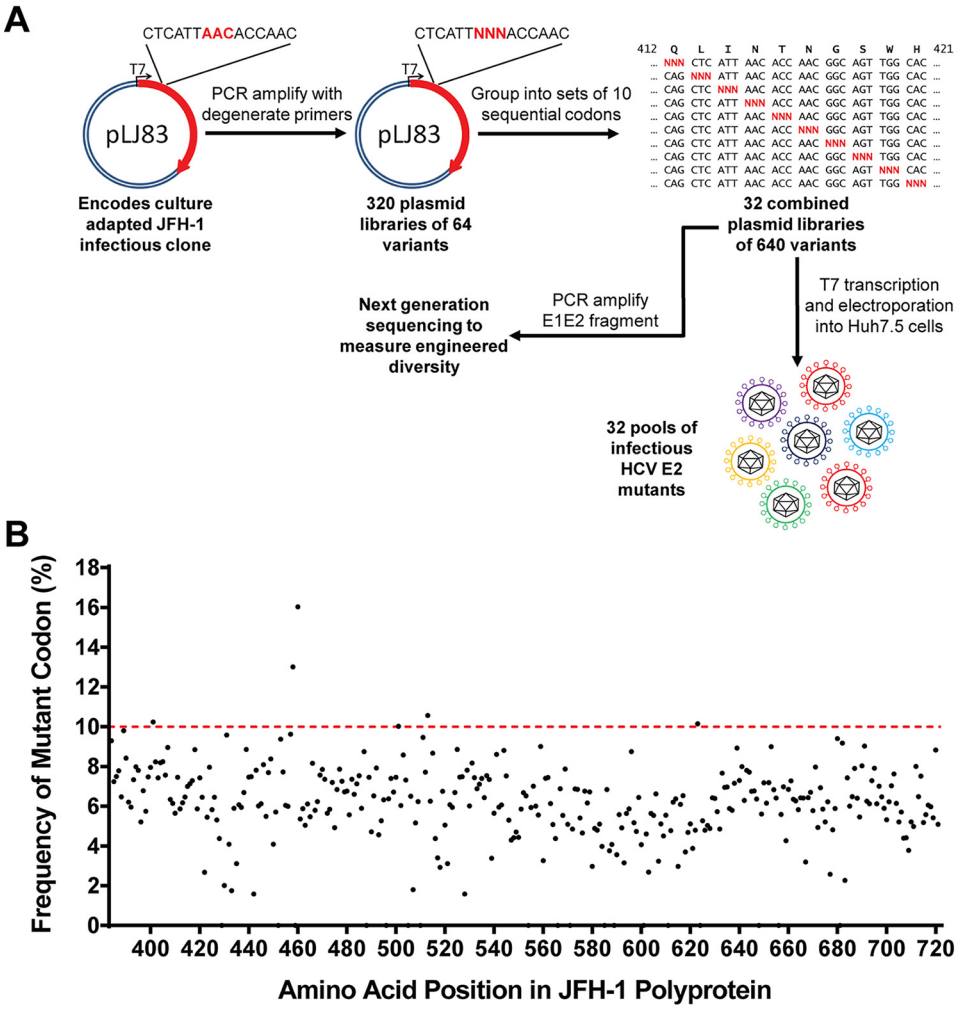

FIG 1 Generation of an SDSM library of infectious HCV and selection of growth-adaptive mutations. (A) Summary of the strategy used to generate the SDSM E2 library. Three hundred twenty degenerate (NNN) primer sets were used to randomize each codon in the ectodomain of E2, excluding cysteine residues. These plasmid libraries were grouped into sets of 10 sequential codons. E1-E2 fragments amplified by PCR from these plasmid pools were used to generate 32 pools of mutant viruses. (B) Amplicon sequencing results for the plasmid libraries. The frequency of mutant codons at each position within the library is shown. The ideal mutant frequency is 10% using our approach (red dashed line).

HCV growth analysis. Huh7.5 cells were infected at a multiplicity of infection (MOI) of 0.1 with parent virus or clonal growth-adapted mutants. Input viruses were removed 6 h postinfection and samples collected every 24 h for 7 days. Viral yield in the supernatant was quantified by FFA. The FFA protocol increased the apparent number of infectious units of growth-adapted virus in a sample slightly because of the more rapid growth and spread to new cells by the mutants. We therefore performed a second growth kinetic analysis using the $TCID_{50}$ method of virus titration to quantify virus. Huh7.5 cells were infected at an MOI of 0.05 with each of the clonal growth-adapted mutants as described above, and viral yield in supernatant was collected 5 days postinfection and calculated.

HCV genome quantification. Quantitative reverse transcription-PCR (qRT-PCR) was used to quantify genome copy number in virus-containing supernatants. Viral RNA was harvested using a QIAamp viral RNA mini-kit (Qiagen). All reactions were prepared using a TaqMan RNA-to-Ct (Applied Biosystems), with forward primer 5′-GATAAACCCACTCTA TGCCCG-3′, reverse primer 5′-CTATCAGGCAGTACCACAAGG-3′, and probe 5′-5′-/56-carboxyfluorescein-CTTTCGCAACCCAACGCTACT CG-36-TAMRASp-3′. Run conditions were 48°C for 15 min, 95°C for 10 min, and then 40 cycles of 95°C for 15 s and 60°C for 1 min. *In vitro*-transcribed genomic transcripts were used as standards.

Inhibition of HCV infection by anti-E2 NMAbs and CD81 large extracellular loop. Two hundred $TCID_{50}$ of parent or mutant viruses were preincubated with a dilution series of anti-E2 antibody or CD81-LEL for 1 h at 37°C and then added to Huh7.5 cells. Infection was quantified 72 h later by FFA, and 50% effective concentrations (EC_{50}) were determined after performing nonlinear regression analysis. Anti-E2 antibodies HC84.26 (a gift of S. Foung, Stanford University) and H77.39 have been described (30, 31). To generate soluble CD81-LEL, residues 114 to 203 of human CD81 were cloned into a Pet28(+)-derived vector with a thrombin-cleavable C-terminal BirA biotinylation site and 6×His tag. CD81-LEL was produced by isopropyl β-D-1-thiogalactopyranoside induction in BL21-DE3 *Escherichia coli* cells and purified by oxidative refolding from inclusion bodies (32). Briefly, bacterial cell pellets were resuspended in a 1:1 mixture of solution buffer (50 mM Tris [pH 8.0], 25% sucrose, 10 mM dithiothreitol [DTT]) and lysis buffer (50 mM Tris [pH 8.0], 1% Triton X-100, 100 mM NaCl, 10 mM DTT). The sample was lysed by sonication and centrifuged, and the pellets were washed three times with wash buffer (50 mM Tris [pH 8.0], 0.5% Triton X-100, 100 mM NaCl, 1 mM DTT) and once in wash buffer without Triton X-100 to obtain purified inclusion bodies. The purified inclusion body pellets were resuspended in TE buffer (10 mM Tris [pH 8.0], 1 mM EDTA), and aliquots of the slurry were

TABLE 1 Mutations selected by serial passage of HCV E2 mutant pools[a]

Position(s) of[b]:		Sites identified by colony sequencing	
Mutation in E2 of P0 virus	P3 putative adaptive mutations identified by consensus sequencing	Amino acid substitution(s) (% of colonies bearing substitution)	Other mutation(s)
404–413	Q412	R (33), A (11), D (3)	I411, L413
414–423	T416	R (16), K (10), N (5), V (5), A (5), G (3), D (3)	I414, N415, N417, G418
445–455	S449	No data[c]	
562–573	T563	V (33), L (33), I (2)	T565
574–583	A579	R (17), L (10), M (7)	
618–628	L619	T (34), E (9), I (2)	W620
	V626	S (15), T (2), Q (2), E (2), R (2)	
629–638	K632	T (62)	I630
639–649	L644	I (32), V (14)	A646

[a] Each pool of E2 mutants was passaged three times in tissue culture. Subsequently, viral RNA was harvested, cDNA generated, and E1-E2 amplified by PCR, and products were Sanger sequenced across the sites of engineered mutations within E2. Eight of the 32 pools had changes to the E2 consensus sequences 404 to 413, 414 to 423, 445 to 455, 563 to 573, 574 to 583, 618 to 628, 629 to 638, and 639 to 649. The E1-E2 fragments from these samples were cloned, and plasmids from individual colonies were sequenced to determine the specific amino acid substitutions selected from each pool.

[b] P0, passage 0; P3, passage 3.

[c] Consensus sequencing suggested only a proline substitution.

solubilized in 6 M guanidine-HCl, 10 mM Tris (pH 8.0), and 20 mM β-mercaptoethanol. Solubilized aliquots were diluted rapidly into a stirring reservoir of oxidative refolding buffer (400 mM L-arginine, 100 mM Tris [pH 8.0], 0.5 mM oxidized glutathione, 5 mM reduced glutathione) followed by overnight incubation. The refolded CD81-LEL then was purified by size exclusion chromatography.

Inhibition of infection by antibodies against HCV entry factors. Huh7.5 cells were treated with serially diluted anti-CD81, anti-claudin-1 (CLDN1), or anti-SR-BI antibody for 1 h at 37°C and then infected with 200 $TCID_{50}$ of parent or mutant viruses. Infection was quantified 72 h later by FFA, and EC_{50} were determined after nonlinear regression analysis. Anti-CD81 (clone JS-81) was purchased from BD Biosciences, and anti-CLDN1 (clone 5.16v5; a gift of I. Hotzel, Genentech) and anti-SR-BI (clone MAb16-71; a gift of A. Nicosia, CEINGE Biotecnologie Avanzate, Naples, Italy) were obtained from colleagues (33, 34).

CRISPR/Cas9-mediated gene editing of SR-BI. To perform CRISPR/Cas9-mediated gene editing, we generated expression plasmids encoding the U6 promoter in front of SR-BI single-guide RNAs (sgRNAs) (35). Two rounds of overlapping PCR were performed by amplifying a guide RNA-carrying plasmid (plasmid 41819 [Addgene]; provided by George Church, Harvard University, Boston, MA). In the first round, PCR products were generated encompassing the U6 promoter through the 5′ end of the guide RNA (consisting of the specific target sequence) with the ME-O-1122 oligonucleotide (5′-CGGGCCCCCCCTCGAGTGTACAAAAAAGCAGGCT-3′) and an SR-BI target sequence-specific reverse oligonucleotide (described below). A second PCR product was generated encompassing a region from the SR-BI target sequence through the end of the guide RNA coding sequence with a forward-direction CLDN1 target sequence-specific oligonucleotide (ME-O-1138; 5′-GCTTCATTCTCGCCTTCCGTTTTAGAGCTAGAAATA-3′). These products were reamplified with only the outside oligonucleotides, ME-O-1122 and ME-O-1123, to produce single PCR products flanked by XhoI and EcoRI sites at the 5′ and 3′ ends, respectively, that were cloned into pBlueScript. Four separate SR-BI-specific gRNA plasmids were created with the following forward and reverse oligonucleotide combinations: ME-O-1241 and -1242, 5′-CTGCTCCGCCAAAGCGCGCGTTTTAGAGCTAGAAATA-3′ and 5′-GCGCGCTTTGGCGGAGCAGCGGTGTTTCGTCCTTTCC-3′; ME-O-1243 and -1244, 5′-GGCCCTACGTGTACAGGTGGTTTTAGAGCTAGAA ATA-3′ and 5′-CACCTGTACACGTAGGGCCCGGTGTTTCGTCCTTTCC-3′; ME-O-1245 and -1246, 5′-CCCTCCAAGTCCCACGGCTGTTTTAGAGCTAGAAATA-3′ and 5′-AGCCGTGGGACTTGGAGGGCGGTGTTTCGTCCTTTCC-3′; and ME-O-1247 and -1248, 5′-GATCCACCTCGTGGACAAGGTTTTAGAGCTAGAAATA-3′ and 5′-CTTGTCCACGAGGTGGATCCGGTGTTTCGTCCTTTCC-3′. They targeted nucleotides 5259 to 5277, 51409 to 51427, 53942 to 53960, and 57068 to 57086 of the SR-BI human genomic locus (relative to GenBank accession number NG_028199), respectively.

Huh7.5 cells were transiently transfected with expression plasmids encoding a human codon-optimized Cas9 protein from *Streptococcus pyogenes* (Addgene plasmid 41815; provided by George Church, Harvard University, Boston, MA) (35) and a pooled mixture of the above-described SR-BI guide RNA expression plasmids. Transfected cells were passaged for 1 to 2 weeks to allow the turnover of previously translated target protein. Cells were then subjected to fluorescence-activated cell sorting (FACS) for loss of SR-BI following staining with the anti-SR-B1 antibody (MAb16-71) and a goat anti-human Alexa-647 antibody (Invitrogen, Carlsbad, CA). Knockout of SR-BI efficiency prior to sorting was 11 to 15%. Single-cell clones were obtained by limiting-dilution cloning in 96-well plates. Individual clones were expanded and assayed for SR-BI expression by flow cytometry with the MAb16-71 antibody, and the capacity to support HCV infection was determined, as previously described (9). We chose Huh7.5 SR-BI^{KO} clone 16 as a representative single-cell clone for further experiments.

Lentiviral transduction of SR-BI^{KO} Huh7.5 cells. Transgene expression through lentiviral transduction was used to complement SR-BI^{KO} cells. To express green fluorescent protein (GFP) alone, the self-inactivating lentiviral provirus TRIP-GFP-linker was used (31). For SR-BI expression, the TRIP-GFP-hu-SR-BI-linker provirus was used. Vesicular stomatitis virus glycoprotein (VSV-G)-pseudotyped lentiviral stocks were produced in 293T cells as previously described (31, 36). Supernatants were collected 2 days posttransfection and used to infect gene-edited Huh7.5 cells, also as previously described (31, 36). Cells were expanded for at least 2 weeks prior to analysis.

Infection of SR-BI gene-edited Huh7.5 cells. Paired infections of control (SR-BIKO+GFP) cells and *trans*-complemented SR-BI knockout cells (termed SR-BI^{KO}+GFP+SR-BI cells) (1×10^5) were plated in wells of a poly-L-lysine-treated 96-well plate 1 day prior to infection. Seventy-five $TCID_{50}$ of virus per well were added, and 3 days later the plates were developed by FFA. Relative infection was calculated by determining the percentage of foci present in SR-BI^{KO}+GFP wells compared to SR-BI^{KO}+GFP+SR-BI wells for each virus.

Virus attachment to gene-edited Huh7.5 cells. SR-BI^{KO}+GFP or SR-BI^{KO}+GFP+SR-BI cells (5×10^5) in suspension were incubated with 5×10^4 $TCID_{50}$ of virus for 3 h on ice. Cells were washed 6 times

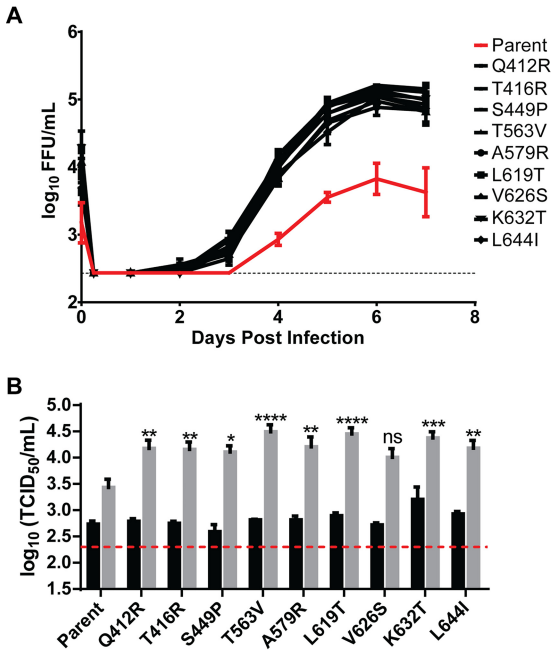

FIG 2 Growth kinetics of viruses bearing the dominant mutations identified by serial passage of E2 mutant pools. (A) Huh7.5 cells were infected with each of the nine mutants selected for study and parent virus at an MOI of 0.1 based on titers calculated using the $TCID_{50}$ method. Input virus was removed 6 h after infection, and samples were collected every 24 h for 7 days. Supernatant viral titers were analyzed by FFA. (B) Cultures of Huh7.5 cells were infected as described for panel A at an MOI of 0.05. Inoculum (black bars) and titers of virus from supernatant at day 5 (gray bars) were determined using the $TCID_{50}$ method. Error bars represent standard errors of the means (SEM), and dashed lines indicate the limit of detection of the assays. Asterisks indicate differences that are statistically significant (*, $P < 0.05$; **, $P < 0.01$; ***, $P < 0.001$; ****, $P < 0.0001$; ns, not significant). The results are averages from three independent experiments performed in duplicate.

with chilled media, and cellular RNA was harvested using a Qiagen RNeasy minikit. Viral genome copies were measured by qRT-PCR as described above. Relative attachment was calculated by determining the percentage of viral RNA bound to SR-BI^{KO}+GFP cells compared to SR-BI^{KO}+GFP+SR-BI cells for each virus.

Sucrose density gradient ultracentrifugation. HCV was ultracentrifuged using 5 to 50% (wt/vol) sucrose gradient ultracentrifugation. Sucrose solutions were prepared in TEN buffer (0.01 M Tris, pH 8.0, 1 mM EDTA, and 100 mM NaCl) using a Gradient Master (Biocomp). The viruses were ultracentrifuged for 17 h at 4°C and 105,000 × *g* (Beckman SW41 Ti), 1-ml fractions were collected, and titers were determined by FFA. The number of genome copies in each fraction was determined by RT-PCR as described above. Fraction densities were measured using an ABBE-3L refractometer (Thermo Fisher Scientific).

Statistical analysis. Statistical analyses were performed using GraphPad Prism software. Differences in mean EC_{50}, relative infection levels, titers, or RNA-to-$TCID_{50}$ ratios between the mutants and parent virus were analyzed by one-way analysis of variance (ANOVA) followed by a Dunnett's test.

RESULTS

Isolation of adaptive JFH-1 variants by passage of a library containing mutagenized E2 genes. Several growth-adaptive mutations have been identified previously in E2, and studying the properties of these mutants is an established method of linking structural features of E2 with functions in the virus life cycle (37–41). Past attempts to identify growth-adaptive mutations in the HCV genome have relied on serial passage of a clonal virus stock for weeks or months until adaptive mutations arise (25, 38–50). To identify adaptive mutations more expediently, we created a library of infectious HCV with a fully mutagenized E2 ectodomain (Fig. 1A). Three hundred twenty primer sets containing three random nucleotides (NNN) corresponding to one codon in the ectodomain of E2 were designed. Using these primers and a JFH-1 infectious clone plasmid, we performed separate SDSM reactions with each primer pair, yielding 320 plasmid libraries. To simplify production of infectious virus, we grouped the plasmid libraries into 32 sets of 10 adjacent codons for all downstream steps. To confirm that each plasmid library contained 64 engineered variants (all nucleotide combinations at each codon), we performed amplicon sequencing of the 32 sets of 10 pooled single-codon plasmid libraries (Fig. 1B). Under ideal conditions, we expected a 10% mutation rate for a single codon within the 10-plasmid pool containing variability at that position; our library had an average mutation rate of 6%. To produce infectious HCV, we transcribed RNA genomes *in vitro* from the pooled plasmids and electroporated each of 32 RNA stocks into Huh7.5 cells. By the end of this process, we had created 32 viral pools, with each containing maximum variability at 10 positions in E2.

Following virus production, cultures of Huh7.5 cells were inoculated with 10^4 $TCID_{50}$ of each of the 32 mutant pools at an MOI of 0.3. Input virus was removed 6 h after infection, and newly produced virus was collected 7 days later. This output virus was used to infect Huh7.5 cells serially twice more, after which Sanger sequencing of HCV E2 RT-PCR products was performed. Eight of the 32 third-passage (P3) viruses had changes in the consensus sequence of E2 within the region containing engineered variability. To determine the specific substitutions that were enriched by passaging, we generated cDNA from P3 viruses and TOPO cloned the E1-E2 genome fragment amplicons produced by PCR. We sequenced the E2 gene for 24 to 48 resultant bacterial colonies from each of the 8 P3 viruses with consensus sequence changes (Table 1).

Based on these results, nine variants that corresponded to the dominant amino acid substitution in each of the P3 viruses were selected for further study: Q412R, T416R, S449P, T563V, A579R,

TABLE 2 Ratios of genome copy number to $TCID_{50}$ for growth-enhanced mutants[a]

Virus	Genome copy per $TCID_{50}$	Fold decrease relative to parent
Parent	7.1×10^3	
Q412R	3.5×10^3	2
T416R	2.7×10^3	2.7
S449P	3.2×10^3	2.2
T563V	1.9×10^3	3.8
A579R	2.4×10^3	2.9
L619T	2.4×10^3	2.9
V626S	3.9×10^3	1.8
K632T	6.3×10^3	1.1
L644I	4.7×10^3	1.5

[a] Huh7.5 cell cultures were infected at an MOI of 0.05 with each mutant and the parental virus. The inoculum was washed off, and 5 days postinfection nascently produced virus was collected and titers were determined by the $TCID_{50}$ method. Genome copies were measured by RT-PCR. Values are the means from three experiments performed in duplicate.

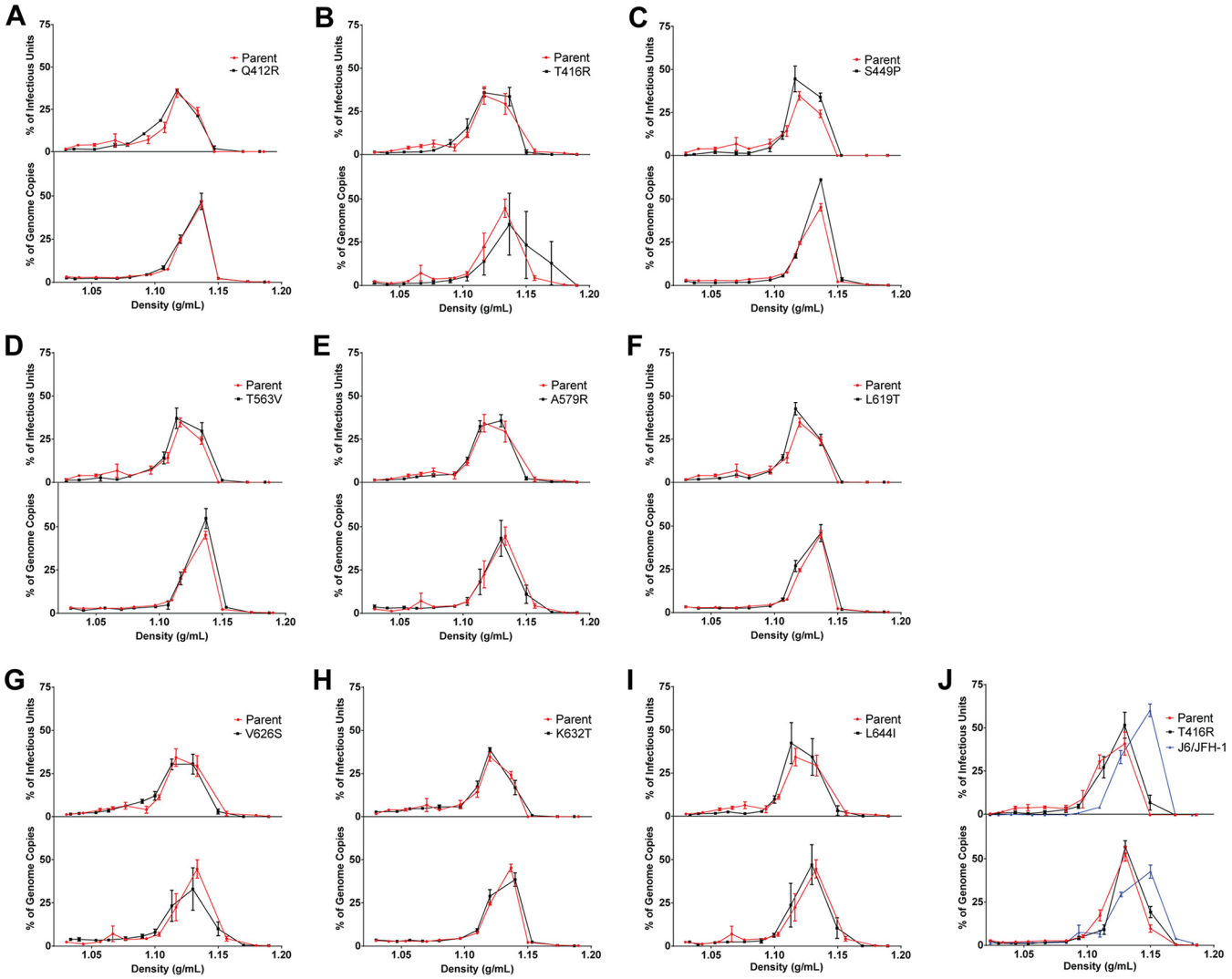

FIG 3 Growth-enhancing mutations do not change buoyant density profiles. Virus-containing medium was layered over 5 to 50% sucrose gradients and ultracentrifuged at 105,000 × *g* for 17 h at 4°C. Twelve 1-ml fractions were collected. The density of the liquid in each fraction was determined using a refractometer, and viral titers and genome copies in each fraction were quantified by FFA and RT-PCR, respectively. In each panel, the percentage of total infectious virus collected in each fraction is displayed in the top graph and the percentage of total genome copies in the bottom, with a control plot for the parental virus shown in red. The mutants are displayed in the panels as Q412R (A), T416R (B), S449P (C), T563V (D), A579R (E), L619T (F), V626S (G), K632T (H), and L644I (I). Panel J includes a comparison between parent JFH-1, the T416R mutant, and J6/JFH-1 viruses run as a control to confirm differences in buoyant density profiles could be measured using our experimental approach. Each point represents means from three independent experiments with error bars representing SEM.

L619T, V626S, K632T, and L644I. Four of these residues (Q412, T416, S449, and T563) are at or very near to positions in E2 that have been reported as adaptive mutations (38–41, 45), with the remainder not having been described to affect growth. Sequencing of individual clones suggested that multiple substitutions at a given position confer a growth advantage over the parent virus with the exception of S449, which had only proline substitutions. S449P also was unique, as it eliminated a predicted N-linked glycosylation site at N448.

Clonal mutant viruses show enhanced growth kinetics. We used conventional site-directed mutagenesis to introduce the nine dominant mutations into the parental infectious clone. Following verification by complete genome sequencing of the plasmids, mutant viruses were generated after electroporation of *in vitro*-derived RNA into Huh7.5 cells, and titers were determined using the $TCID_{50}$ method. To validate the significance of the mutations, multistep viral growth analyses were performed by FFA after infection of Huh7.5 cells (MOI of 0.1) with each mutant and the parental virus (Fig. 2A). Whereas each of the mutations conferred a growth advantage compared to the parental virus, we noticed that the input virus titer ($t = 0$) for all of the mutant viruses appeared higher than that of the parent, JFH-1, in this assay. Because we inoculated with equivalent input amounts based on the $TCID_{50}$ assay, we hypothesized that the difference at $t = 0$ of the input virus reflected the more rapid growth of the adaptive mutant strains over the course of the FFA compared to WT virus. Given this potential confounding issue, we performed a second confirmatory viral growth assay. Cultures of Huh7.5 cells were

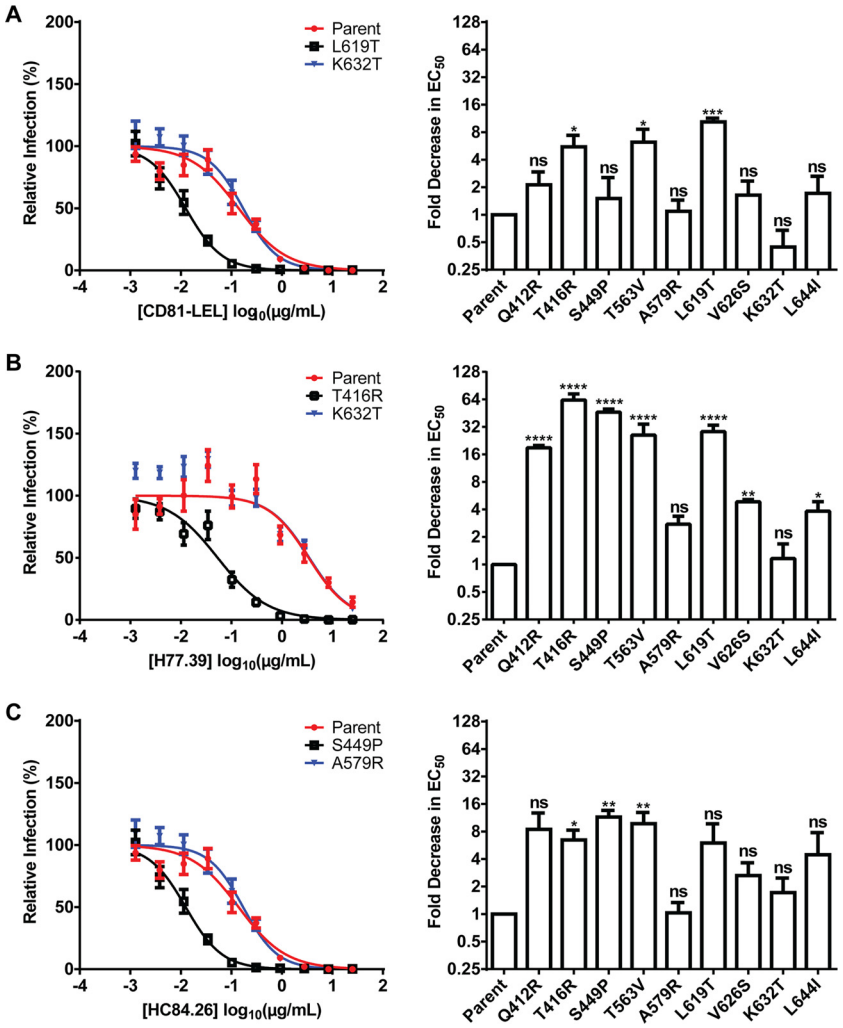

FIG 4 Subset of growth-enhanced mutants are more sensitive to CD81-LEL and NMAb inhibition. Parental or mutant viruses were preincubated with a dilution series of CD81-LEL (A) or anti-E2 antibody H77.39 (B) or HC84.26 (C) for 1 h at 37°C and then added to Huh7.5 cells. Infection was quantified 72 h later by FFA. EC_{50} were determined by nonlinear regression analysis. The panels on the left are representative dose-response curves for parental virus and the mutants. The fold decrease in EC_{50} for the antibody treatment of mutant relative to parental virus is plotted on the right. Asterisks indicate differences that are statistically significant (*, $P < 0.05$; **, $P < 0.01$; ***, $P < 0.001$; ****, $P < 0.0001$; ns, not significant). Error bars represent SEM. The results are the averages from three independent experiments performed in triplicate or quadruplicate.

infected at an MOI of 0.05 (as determined by $TCID_{50}$ assay) with the mutant and parent viruses, supernatants were collected 5 days later, and titers were determined by $TCID_{50}$ assay (Fig. 2B). Using this second method, the mutants exhibited a 5- to 10-fold growth advantage compared to the parental viruses. In this assay, the V626S mutant did not show a statistically significant growth advantage compared to the parental strains. Nonetheless, it may still be a growth-adaptive mutation based on accumulated data (Table 1 and Fig. 2).

Particle-to-infectious-unit ratios for E2 mutants. We next explored whether there were functional differences in the properties of growth-adapted viruses compared to the parent JFH-1 strain. We initially assessed the relative specific infectivity by measuring the RNA-to-$TCID_{50}$ ratio of each mutant virus (Table 2). A more efficient assembly process or increased stability of infectious virions could contribute to increased peak titers. As HCV growth kinetic assays are long, small differences may compound over time and account for at least part of the adaptive growth phenotype. Using the titered samples described for Fig. 2B, viral RNA was harvested and genome copy determined via RT-PCR using *in vitro*-derived RNA from infectious clone plasmids as standards. The greatest difference between the parent and a mutant virus was observed for T563V, and even this fold change was less than 4-fold. All mutant viruses, apart from K632T, had a lower RNA-to-$TCID_{50}$ ratio than the parental virus, although these differences did not achieve statistical significance.

Buoyant density profiles of growth-adapted mutants are similar to that of the parent. HCV has a unique buoyant density profile compared to many other *Flaviviridae* family members (e.g., flaviviruses). Because of lipoprotein incorporation, infectious HCV particles have a lower density and broader infectivity peak (3, 4). Some E2 growth variants have altered buoyant density profiles relative to their parental strains (37, 40), and such differences may reflect alterations in lipoprotein incorporation or

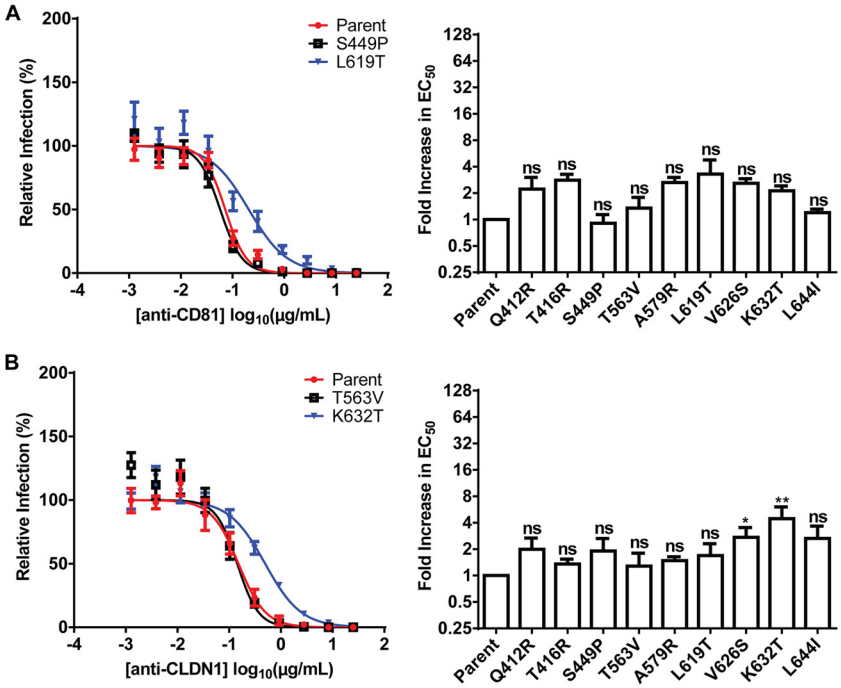

FIG 5 Dependence on CD81 and CLDN1 for growth-adapted mutants is similar to that of the parental virus. Huh7.5 cells were preincubated with a dilution series of anti-CD81 (A) or anti-CLDN1 (B) for 1 h at 37°C and then infected with parental and growth-adapted mutant viruses. Infection was quantified 72 h later by FFA and EC_{50} determined by nonlinear regression. For each mutant virus, the fold change in EC_{50} for the antibody treatment relative to parental virus is plotted. Asterisks indicate differences that are statistically significant (*, $P < 0.05$; **, $P < 0.01$; ns, not significant). Error bars represent SEM. The results are averages from three independent experiments performed in triplicate or quadruplicate.

changes to the subset of HCV particles (high or low density) that display peak infectivity for a variant. To determine whether our panel of mutants had shifts in buoyant density profiles, we performed sucrose gradient ultracentrifugation and quantified the density, viral titer, and HCV genome copy number in each fraction collected (Fig. 3). The mutants all behaved similarly to parent virus, suggesting they have similar lipoprotein utilization or incorporation.

Some adaptive mutations enhance CD81-LEL and NMAb sensitivity. E2 is the major viral target of neutralizing antibodies during infection. Many of the most effective broadly NMAbs block interaction between E2 and CD81, one of the key HCV entry receptors (30, 31, 51, 52). Some growth-adaptive mutations in E2 were shown to increase inhibition by soluble CD81-LEL and NMAbs (37, 39, 40). To assess whether the identified mutations affected the binding of E2 to CD81, we performed inhibition of infection assays with a soluble CD81-LEL (Fig. 4A). A subset of adaptive mutant viruses (T416R, T563V, and L619T) were inhibited more efficiently by CD81-LEL than the parent JFH-1 virus (>5-fold decrease in EC_{50}; $P < 0.05$); thus, an enhanced CD81-E2 interaction might contribute to the growth advantages of these viruses. However, most of the mutants were not more sensitive to CD81-LEL inhibition, which contrasts with some published growth-adaptive variants.

We next performed dose-response inhibition of infection assays with two broadly neutralizing anti-E2 NMAbs, H77.39 (Fig. 4B) and HC84.26 (Fig. 4C), both of which block interactions between E2 and CD81 (30, 31). H77.39 maps to an epitope centered on amino acids 415 and 417 and part of a larger epitope between positions 412 and 421. Residues within this region, especially W420, can influence CD81 interactions (24, 39). HC84.26 maps to conserved residues within the CD81 binding site between residues 441 and 446 and to residue 620 (H77 residue numbers). Q412R, T416R, S449P, T563V, and L619T viruses were neutralized more efficiently by H77.39 than the parent, JFH-1 (>5-fold decrease in EC_{50}; $P < 0.0001$) (Fig. 4B), and T416R, S449P, and T563V viruses were inhibited to a greater extent (>5-fold decrease in EC_{50}; $P < 0.05$) by HC84.26 (Fig. 4C). However, A579R, V626S, K632T, and L644I viruses were unchanged or exhibited modestly shifted profiles with anti-E2 NMAbs and CD81-LEL.

HCV containing E2 adaptive mutations require CD81 and CLDN1 for infection. HCV entry is a complex process that requires several host factors, including heparan sulfate proteoglycans (53, 54), low-density lipoprotein receptor (54–56), SR-BI (21, 57), CD81 (51, 58), CLDN1 (59), and occludin (OCLN) (60). Some E1 and E2 mutations cause altered entry factor usage or reduce dependence on a particular receptor (37, 39, 40, 61). To test whether our adaptive mutations changed CD81 or CLDN1 receptor dependency, we performed neutralization assays with antibodies against these host entry factors. However, all of the adaptive mutant viruses were inhibited by anti-CD81 and anti-CLDN1 similarly to the parental strain, suggesting little change in dependency on these receptors (Fig. 5).

Growth-adaptive mutants are less dependent on SR-BI for infection. Markedly different neutralization profiles were observed for the mutants when an anti-SR-BI antibody was used (Fig. 6), as each variant was more resistant to antibody inhibition. Whereas the parental JFH-1 had a lower asymptote of 14% relative infection (i.e., resistant fraction), some mutant viruses appeared to be entirely resistant to anti-SR-BI treatment of Huh7.5 cells.

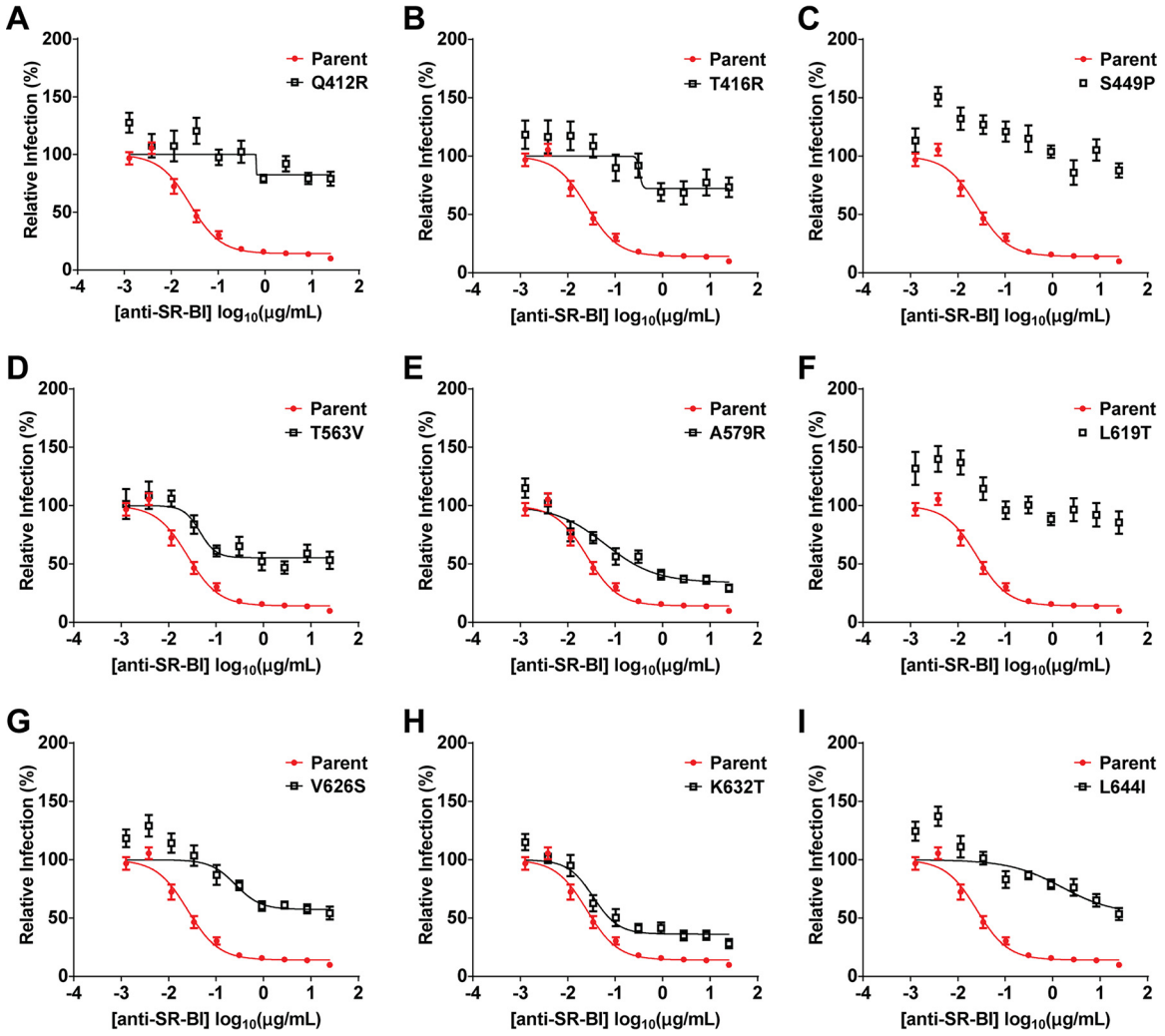

FIG 6 Growth-enhanced mutants are less dependent on SR-BI for infection. Huh7.5 cells were preincubated with a dilution series of anti-SR-BI for 1 h at 37°C and then infected with parental and mutant viruses. Infection was quantified 72 h later by FFA. In each panel, the dose-response curve for a single mutant virus is displayed with the same control dose-response curve as that for parental virus. The mutants are displayed in the panels as Q412R (A), T416R (B), S449P (C), T563V (D), A579R (E), L619T (F), V626S (G), K632T (H), and L644I (I). Error bars represent SEM. The results are averages from three independent experiments performed in quadruplicate.

Even the most sensitive mutant virus had a lower asymptote at 34% relative infection, 2.5-fold greater than the parent. To confirm changes to SR-BI dependency, we generated SR-BI^{KO} Huh7.5 cells using CRISPR/Cas9 gene editing (Fig. 7). A clonal SR-BI^{KO} Huh7.5 line, clone 16, was selected for further study. Clone 16 was confirmed to lack SR-BI expression (Fig. 7A) and exhibited a moderately impaired capacity to support HCV cell entry (Fig. 7B). Importantly, this phenotype was restored completely by *trans*-complementation from a lentiviral vector (Fig. 7B). Paired infections of control (GFP) and SR-BI (SR-BI+GFP) *trans*-complemented SR-BI^{KO} cells with WT and mutant HCV corroborated the anti-SR-BI antibody data: the mutants showed greater infection in cells lacking SR-BI than the parental virus (Fig. 7C). Thus, growth adaptation in Huh7.5 cells resulted in the emergence of viruses with less dependency on SR-BI for infection. To assess whether the mutations had a similar effect on other HCV genotypes, we generated homologous mutations to JFH-1 S449P, L619T, and L644I in a chimeric infectious clone encoding the structural genes of the genotype 1 H77 isolate (H77/JFH-1). We performed paired infections of control and SR-BI *trans*-complemented SR-BI^{KO} cells with the H77/JFH-1 mutants and again observed less dependence on SR-BI for infection with the mutant viruses (Fig. 7D). Finally, we explored whether deletion of SR-BI from Huh7.5 cells differentially affected the attachment of parent and mutant viruses. Notably, the attachment of all viruses to the SR-BI gene-edited cells was similar, suggesting the mutations affect a postattachment interaction step that requires SR-BI (Fig. 7E).

Our results suggested that all of the growth-adaptive mutations identified in our screen modulated the SR-BI dependence of HCV for entry into target cells. When we mapped the positions of the growth-adaptive mutations on the E2 core structure (19), we found that four of the residues (L619T, V626S, K632T, and L644I) were proximal to one another, with K632T and L644I directly adjacent in an antiparallel beta hairpin (Fig. 7F). This clustering suggests a role for this region of E2 in an interaction with SR-BI.

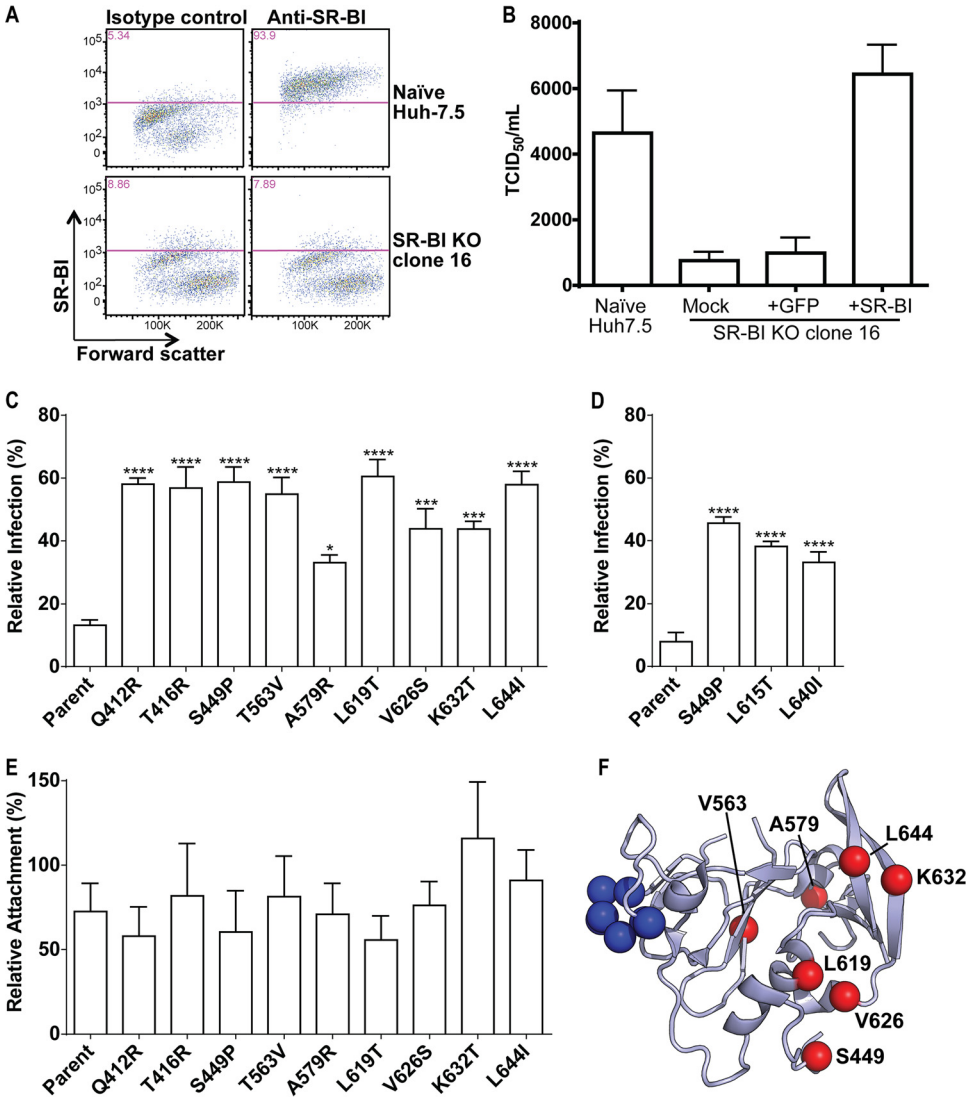

FIG 7 Generation of SR-BI-deficient Huh7.5 cells. (A) Parental Huh7.5 cells or Huh7.5 SR-BI^{KO} clone cell populations were stained with isotype control or SR-BI-specific antibodies and analyzed by flow cytometry. (B) The relative titers of a single stock of HCV were determined by limiting dilution assay on parental Huh7.5 cells or Huh7.5 SR-BI^{KO} clonal cells either not expressing a transgene (mock) or transduced with lentiviral particles to express GFP or SR-BI. Values represent the mean $TCID_{50}$/ml, and the error bars indicate SEM from three independent assays. (C) SR-BI^{KO} Huh7.5 cells stably expressing GFP or GFP and SR-BI were infected with parental or variant virus. The relative infection of GFP-only cells compared to GFP- and SR-BI-coexpressing cells is shown. Error bars represent SEM. Asterisks indicate differences that are statistically significant (*, $P < 0.05$; ***, $P < 0.001$; ****, $P < 0.0001$). The results are averages from three independent experiments performed in quadruplicate. (D) SR-BI^{KO} Huh7.5 cells stably expressing GFP or GFP and SR-BI were infected as described for panel C using parental H77/JFH-1 and H77/JFH-1 variant viruses bearing corresponding mutations to JFH-1 S449P, L619T, and L644: S449P, L615T, and L640L, respectively. (E) SR-BI^{KO} Huh7.5 cells stably expressing GFP or GFP and SRBI were incubated with parental or variant virus for 3 h on ice. Cells were washed extensively, cellular RNA was harvested, and HCV genome copies were quantified by qRT-PCR. The relative attachment to GFP-only cells compared to GFP- and SR-BI-coexpressing cells is shown. Error bars represent SEM. No statistically significant differences were observed. The results are averages from three independent experiments performed in duplicate. (F) Ribbon diagram of the E2 core structure (PDB entry 4MWF) (19) illustrating the locations of the adaptive mutations identified in this study (red spheres) and residues essential for CD81 binding (blue spheres; amino acid positions 529 to 535). Q412 and T416 were excluded as they fall within a disordered region.

DISCUSSION

The study of single-amino-acid viral variants has facilitated advances in our understanding of host-pathogen interactions. However, classical methods of producing viral variants rely on stochastic errors of the viral polymerase to generate mutations. Such approaches can be an inefficient means of producing new mutants even when selective pressure is applied. This approach may fail to explore all possible amino acid substitutions, as multiple nucleotide changes at a single codon are less likely. The limitation of relying on randomly occurring mutations is particularly problematic for HCV, as it is relatively slow growing in culture. By molecularly engineering variability into E2 and producing our SDSM library, we circumvented the need to wait months for mutations to arise in culture. Where previous attempts to identify new culture-adaptive mutations yielded few mutations, we selected for many variants within three tissue culture passages.

TABLE 3 Number of genotype 2 sequences in the ViPR database bearing each amino acid at the site of adaptive mutation[a]

Amino acid	No. of genotype 2 sequences in virus:								
	Q412R	T416R	S449P	T563V	A579R	L619T	V626S	K632T	L644I
Ala (A)	4	33	1,338	1	252				
Arg (R)	31		1		9			1	
Asn (N)	136	82	1						
Asp (D)	13	2	212						
Cys (C)							1		
Gln (Q)	3,986		1		1			4	
Glu (E)	181	110	2		1				
Gly (G)	9		3		11			1	
His (H)	36		1		3				
Ile (I)	2			1			7		1
Leu (L)	4		117			469	9		417
Lys (K)	5	8	4					460	
Met (M)	12	1							6
Phe (F)		1					2		41
Pro (P)	45	2	3						
Ser (S)	231	803	1,868		220		1		
Thr (T)	28	3,211	5	528	12		1		
Trp (W)	14								
Tyr (Y)									
Val (V)				1	3		444		1
Total	4,737	4,253	3,556	531	512	469	465	466	466

[a] All HCV genotype 2 E2 amino acid sequences in the ViPR database were aligned, and the number of sequences containing each residue at the sites of our adaptive mutations was determined.

Previous studies of growth-enhancing E2 mutations were limited to a few sites with E2, between positions 412 and 421 and at positions 451 and 563 (38–41). These mutations increased the sensitivity of the virus to inhibition by CD81-LEL and anti-HCV NMAbs targeting the E2-CD81 interaction. These mutations may elicit a more open E2 conformation, which promotes interactions with CD81 or other entry factors at the cost of greater exposure of the NMAbs that block access to the CD81 binding site on E2. Additionally, some of these prior mutations altered the dependence of HCV on SR-BI and caused a shift in the buoyant density profile of the infectious viruses. In comparison, our panel of mutations was distributed more evenly across the E2 protein. Four substitutions (Q412R, T416R, S449P, and T563V) were proximal to the previously described positions; however, the remaining five mutations (A579R, L619T, V626S, K632T, and L644I) were at unique positions within E2.

The increased sensitivity to NMAb and CD81-LEL inhibition by growth-enhancing E2 mutations may represent a trade-off made by the virus in the face of humoral immune pressure, with a compromise in growth kinetics to facilitate immune evasion. Consistent with this hypothesis, an alignment of all genotype 2 E2 amino acid sequences in the ViPR database (http://www.viprbrc.org/) revealed that our adaptive mutations were present at low frequencies or absent from most HCV isolates (Table 3). A subset of our mutations, Q412R, T416R, S449P, T563V, and L619T, were more sensitive to NMAb inhibition than the parental virus. Of these, T416R, T563V, and L619T also were more sensitive to inhibition by CD81-LEL. T416R falls within the epitope of H77.39 and correspondingly is neutralized more efficiently by this antibody. The S449P mutation eliminates a predicted N-linked glycosylation site at N448 near the CD81 binding site, which might enhance NMAb potency by reducing steric hindrance of the glycan. At present, the effects of other residues on the potency of neutralization by H77.39 and HC84.26 are more challenging to model. Structural data for the binding of these antibodies to E2 are not available, and some of the residues are not visible in the crystal structures of the E2 core. Residues that are not proximal to the footprints of H77.39 and HC84.26 could affect neutralization potency indirectly, perhaps via altered lipoprotein association or changes in the global conformation of E2.

Q412R and S449P were more sensitive to H77.39 and HC84.26 antibody neutralization without showing increased inhibition by CD81-LEL. This suggests that increased exposure of the CD81 binding site is not responsible exclusively for enhanced anti-E2 neutralization. We also identified growth-adaptive mutations in E2 (e.g., A579R and K632T) that did not render the virus more susceptible to neutralizing antibodies, although further studies are warranted. These mutants could be more sensitive to NMAbs targeting different epitopes. Alternatively, these mutations may adapt the virus to Huh7.5 cells but not to cell targets *in vivo*.

Mutations in E1 and E2 can alter the dependence of HCV on particular receptors or even cause a shift in receptor utilization (37, 39, 40, 61). We tested whether our growth-adapted viruses had different entry factor utilizations. Antibodies to CD81 and CLDN1 showed little difference in potency between the mutant and parental viruses; thus, the mutant viruses remained dependent on CD81 and CLDN1 for entry. A different pattern was observed when cells were pretreated with anti-SR-BI antibodies. Parental virus was neutralized efficiently with a 90% reduction at high antibody concentrations. However, all of the growth-adapted viruses were resistant to the effects of anti-SR-BI, a finding which was corroborated using CRISPR/Cas9-generated SR-BI^{KO} and *trans*-complemented cells. Additionally, H77/JFH-1 clones bearing homologous mutations to JFH-1 S449P, L619T,

TABLE 4 Summary of properties of the growth-adaptive E2 variants[a]

Virus	H77 residue	Fold decrease in RNA-to-$TCID_{50}$ ratio[b]	Fold change in EC_{50}[c]					Antibody dose response[d] (% resistant)	
			H77.39*	HC84.26*	CD81-LEL*	Anti-CD81**	Anti-CLDN1**	Anti-SR-BI	$SR\text{-}BI^{KO}$
Q412R	Q412	1.7	19	8.4	2.1	2.2	2.0	82	58
T416R	T416	2.3	63	6.5	5.5	2.8	1.4	72	57
S449P	S449	2.0	46	11	1.5	0.91	1.9	100	59
T563V	T561	3.3	26	9.7	6.2	1.4	1.3	55	55
A579R	(N577)	3.8	2.8	1.0	1.1	2.6	1.5	34	33
L619T	L615	2.6	28	6.0	10	3.3	1.7	100	61
V626S	I622	1.5	4.9	2.6	1.6	2.6	2.7	57	44
K632T	K628	1.2	1.2	1.7	0.44	2.1	4.4	36	44
L644I	L640	1.3	3.8	4.5	1.7	1.2	2.7	53	58

[a] A summary of the properties of the mutants identified in this study.
[b] Fold decrease relative to parent is listed for the RNA-to-$TCID_{50}$ ratio.
[c] The fold change in EC_{50} (increase or decrease) is listed for all dose-response inhibition assays. *, fold decrease; **, fold increase.
[d] For the SR-BI antibody dose response or infection of $SR\text{-}BI^{KO}$ cells, the percentage of virus resistant to SR-BI blockade or deletion is listed.

and L644I similarly were resistant to SR-BI deletion, suggesting the mutations have a conserved role in modulating the SR-BI interaction. As changes to lipoprotein incorporation could contribute to the observed SR-BI phenotype of some growth-adaptive mutants, we analyzed buoyant density profiles for relative infectivity. However, all of our growth-adaptive mutants had virtually identical profiles relative to parental virus. This observation suggests that the altered SR-BI usage is not a function of changes to lipoprotein incorporation. Consistent with this idea, HCV uses SR-BI at multiple points in the entry pathway as an attachment factor via interactions with virus-associated lipoprotein and also during postattachment steps by directly interacting with E2 (62). As deletion of SR-BI did not differentially affect attachment of parent or variant HCV to Huh7.5 cells, these mutations may alter a postattachment interaction with SR-BI.

While it is known that deletion of HVR1 abrogates binding of E2 to SR-BI, the details of this interaction remain unclear. Our findings, along with data from previous studies, suggest that reduced SR-BI dependence for infection is a common feature of growth-enhancing E2 mutations (at least in cell culture) and that residues distributed across the E2 protein can modulate the interaction with SR-BI. As four of the sites of growth-adaptive mutations we identified with altered SR-BI dependency were proximal to each other, we speculate this represents part of a possible SR-BI binding site in E2. The molecular basis for why our mutants show less dependency on SR-BI awaits more detailed structural or biochemical resolution of the E2 and SR-BI interaction.

In summary, we developed a novel E2 JFH-1 mutant library with significant diversity and used it to identify new growth-adaptive mutations for study. The properties of these mutants are summarized in Table 4 and varied with respect to NMAb and CD81-LEL inhibition sensitivity and SR-BI dependence. More broadly, these results demonstrate the utility of libraries of variant viruses to address questions in HCV biology, especially as it relates to receptor interactions and, possibly, immune escape. The SDSM method provides a depth of variability that can be employed rapidly for discovery of novel HCV variants with unique functional profiles.

ACKNOWLEDGMENTS

We thank the Genome Technology Access Center in the Department of Genetics at Washington University School of Medicine for help with genomic analysis. The Center is partially supported by an NCI Cancer Center Support Grant (P30 CA91842) to the Siteman Cancer Center and by ICTS/CTSA (UL1 TR000448) from the National Center for Research Resources (NCRR), a component of the National Institutes of Health (NIH), and NIH Roadmap for Medical Research.

M.J.E. was supported by the National Institutes of Health/National Institute of Diabetes and Digestive and Kidney Diseases (R01 DK095125), the American Cancer Society (RSG-12-176-01-MPC), the Pew Charitable Funds, and the Burroughs Wellcome Fund.

FUNDING INFORMATION

This work, including the efforts of Matthew J. Evans, was funded by HHS | NIH | National Institute of Diabetes and Digestive and Kidney Diseases (NIDDK) (R01 DK095125).

REFERENCES

1. **Mohd Hanafiah K, Groeger J, Flaxman AD, Wiersma ST.** 2013. Global epidemiology of hepatitis C virus infection: new estimates of age-specific antibody to HCV seroprevalence. Hepatology **57:**1333–1342. http://dx.doi.org/10.1002/hep.26141.
2. **Hajarizadeh B, Grebely J, Dore GJ.** 2013. Epidemiology and natural history of HCV infection. Nat Rev Gastroenterol Hepatol **10:**553–562. http://dx.doi.org/10.1038/nrgastro.2013.107.
3. **Thomssen R, Bonk S, Propfe C, Heermann KH, Köchel HG, Uy A.** 1992. Association of hepatitis C virus in human sera with beta-lipoprotein. Med Microbiol Immunol **181:**293–300. http://dx.doi.org/10.1007/BF00198849.
4. **Nielsen SU, Bassendine MF, Burt AD, Martin C, Pumeechockchai W, Geoffrey L, Toms GL.** 2006. Association between hepatitis C virus and very-low-density lipoprotein (VLDL)/LDL analyzed in iodixanol density gradients association between hepatitis C virus and very-low-density lipoprotein (VLDL)/LDL analyzed in iodixanol density gradients. J Virol **80:**2418–2428. http://dx.doi.org/10.1128/JVI.80.5.2418-2428.2006.
5. **Smith DB, Bukh J, Kuiken C, Muerhoff AS, Rice CM, Stapleton JT, Simmonds P.** 2013. Expanded classification of hepatitis C virus into 7 genotypes and 67 subtypes: updated criteria and assignment web resource. Hepatology **59:**318–327. http://dx.doi.org/10.1002/hep.26744.
6. **Saeed M, Andreo U, Chung H-Y, Espiritu C, Branch AD, Silva JM, Rice CM.** 2015. SEC14L2 enables pan-genotype HCV replication in cell culture. Nature **524:**471–475. http://dx.doi.org/10.1038/nature14899.
7. **Zhong J, Gastaminza P, Cheng G, Kapadia S, Kato T, Burton DR, Wieland SF, Uprichard SL, Wakita T, Chisari FV.** 2005. Robust hepatitis C virus infection in vitro. Proc Natl Acad Sci U S A **102:**9294–9299. http://dx.doi.org/10.1073/pnas.0503596102.

8. **Wakita T, Pietschmann T, Kato T, Date T, Miyamoto M, Zhao Z, Murthy K, Habermann A, Kräusslich H-G, Mizokami M, Bartenschlager R, Liang TJ.** 2005. Production of infectious hepatitis C virus in tissue culture from a cloned viral genome. Nat Med **11:**791–796. http://dx.doi.org/10.1038/nm1268.
9. **Lindenbach BD, Evans MJ, Syder AJ, Wölk B, Tellinghuisen TL, Liu CC, Maruyama T, Hynes RO, Burton DR, McKeating JA, Rice CM.** 2005. Complete replication of hepatitis C virus in cell culture. Science **309:**623–626. http://dx.doi.org/10.1126/science.1114016.
10. **Li Y-P, Ramirez S, Jensen SB, Purcell RH, Gottwein JM, Bukh J.** 2012. Highly efficient full-length hepatitis C virus genotype 1 (strain TN) infectious culture system. Proc Natl Acad Sci U S A **109:**19757–19762. http://dx.doi.org/10.1073/pnas.1218260109.
11. **Li Y-P, Ramirez S, Gottwein JM, Scheel TKH, Mikkelsen L, Purcell RH, Bukh J.** 2012. Robust full-length hepatitis C virus genotype 2a and 2b infectious cultures using mutations identified by a systematic approach applicable to patient strains. Proc Natl Acad Sci U S A **109:**E1101–E1110. http://dx.doi.org/10.1073/pnas.1203829109.
12. **Li Y-P, Ramirez S, Mikkelsen L, Bukh J.** 2015. Efficient infectious cell culture systems of the hepatitis C virus (HCV) prototype strains HCV-1 and H77. J Virol **89:**811–823. http://dx.doi.org/10.1128/JVI.02877-14.
13. **Kim S, Date T, Yokokawa H, Kono T, Aizaki H, Maurel P, Gondeau C, Wakita T.** 2014. Development of hepatitis C virus genotype 3a cell culture system. Hepatology **60:**1838–1850. http://dx.doi.org/10.1002/hep.27197.
14. **Farci P, Shimoda A, Coiana A, Diaz G, Peddis G, Melpolder JC, Strazzera A, Chien DY, Munoz SJ, Balestrieri A, Purcell RH, Alter HJ.** 2000. The outcome of acute hepatitis C predicted by the evolution of the viral quasispecies. Science **288:**339–344. http://dx.doi.org/10.1126/science.288.5464.339.
15. **Liu L, Fisher BE, Dowd KA, Astemborski J, Cox AL, Ray SC.** 2010. Acceleration of hepatitis C virus envelope evolution in humans is consistent with progressive humoral immune selection during the transition from acute to chronic infection. J Virol **84:**5067–5077. http://dx.doi.org/10.1128/JVI.02265-09.
16. **Lindenbach BD, Rice CM.** 2013. The ins and outs of hepatitis C virus entry and assembly. Nat Rev Microbiol **11:**688–700. http://dx.doi.org/10.1038/nrmicro3098.
17. **Falson P, Bartosch B, Alsaleh K, Tews BA, Loquet A, Ciczora Y, Riva L, Montigny C, Montpellier C, Duverlie G, Pécheur E-I, le Maire M, Cosset F-L, Dubuisson J, Penin F.** 2015. Hepatitis C virus envelope glycoprotein E1 forms trimers at the surface of the virion. J Virol **89:**10333–10346. http://dx.doi.org/10.1128/JVI.00991-15.
18. **Vieyres G, Thomas X, Descamps V, Duverlie G, Patel AH, Dubuisson J.** 2010. Characterization of the envelope glycoproteins associated with infectious hepatitis C virus. J Virol **84:**10159–10168. http://dx.doi.org/10.1128/JVI.01180-10.
19. **Kong L, Giang E, Nieusma T, Kadam RU, Cogburn KE, Hua Y, Dai X, Stanfield RL, Burton DR, Ward AB, Wilson IA, Law M.** 2013. Hepatitis C virus E2 envelope glycoprotein core structure. Science **342:**1090–1094. http://dx.doi.org/10.1126/science.1243876.
20. **Khan AG, Whidby J, Miller MT, Scarborough H, Zatorski AV, Cygan A, Price AA, Yost SA, Bohannon CD, Jacob J, Grakoui A, Marcotrigiano J.** 2014. Structure of the core ectodomain of the hepatitis C virus envelope glycoprotein 2. Nature **509:**381–384. http://dx.doi.org/10.1038/nature13117.
21. **Scarselli E, Ansuini H, Cerino R, Roccasecca RM, Acali S, Filocamo G, Traboni C, Nicosia A, Cortese R, Vitelli A.** 2002. The human scavenger receptor class B type I is a novel candidate receptor for the hepatitis C virus. EMBO J **21:**5017–5025. http://dx.doi.org/10.1093/emboj/cdf529.
22. **Bankwitz D, Steinmann E, Bitzegeio J, Ciesek S, Friesland M, Herrmann E, Zeisel MB, Baumert TF, Keck Z, Foung SKH, Pécheur E-I, Pietschmann T.** 2010. Hepatitis C virus hypervariable region 1 modulates receptor interactions, conceals the CD81 binding site, and protects conserved neutralizing epitopes. J Virol **84:**5751–5763. http://dx.doi.org/10.1128/JVI.02200-09.
23. **Drummer HE, Boo I, Maerz AL, Poumbourios P.** 2006. A conserved Gly436-Trp-Leu-Ala-Gly-Leu-Phe-Tyr motif in hepatitis C virus glycoprotein E2 is a determinant of CD81 binding and viral entry. J Virol **80:**7844–7853. http://dx.doi.org/10.1128/JVI.00029-06.
24. **Owsianka AM, Timms JM, Tarr AW, Brown RJP, Hickling TP, Szwejk A, Bienkowska-Szewczyk K, Thomson BJ, Patel AH, Ball JK.** 2006. Identification of conserved residues in the E2 envelope glycoprotein of the hepatitis C virus that are critical for CD81 binding. J Virol **80:**8695–8704. http://dx.doi.org/10.1128/JVI.00271-06.
25. **Jiang J, Luo G.** 2012. Cell culture-adaptive mutations promote viral protein-protein interactions and morphogenesis of infectious hepatitis C virus. J Virol **86:**8987–8997. http://dx.doi.org/10.1128/JVI.00004-12.
26. **Kato T, Furusaka A, Miyamoto M, Date T, Yasui K, Hiramoto J, Nagayama K, Tanaka T, Wakita T.** 2001. Sequence analysis of hepatitis C virus isolated from a fulminant hepatitis patient. J Med Virol **64:**334–339. http://dx.doi.org/10.1002/jmv.1055.
27. **Reed LJ, Muench H.** 1938. A simple method of estimating fifty per cent endpoints. Am J Hyg (Lond) **27:**493–497.
28. **Yi M, Ma Y, Yates J, Lemon SM.** 2007. Compensatory mutations in E1, p7, NS2, and NS3 enhance yields of cell culture-infectious intergenotypic chimeric hepatitis C virus. J Virol **81:**629–638. http://dx.doi.org/10.1128/JVI.01890-06.
29. **Pickett BE, Sadat EL, Zhang Y, Noronha JM, Squires RB, Hunt V, Liu M, Kumar S, Zaremba S, Gu Z, Zhou L, Larson CN, Dietrich J, Klem EB, Scheuermann RH.** 2012. ViPR: an open bioinformatics database and analysis resource for virology research. Nucleic Acids Res **40:**593–598.
30. **Keck Z, Xia J, Wang Y, Wang W, Krey T, Prentoe J, Carlsen T, Li AY-J, Patel AH, Lemon SM, Bukh J, Rey FA, Foung SKH.** 2012. Human monoclonal antibodies to a novel cluster of conformational epitopes on HCV E2 with resistance to neutralization escape in a genotype 2a isolate. PLoS Pathog **8:**e1002653. http://dx.doi.org/10.1371/journal.ppat.1002653.
31. **Sabo MC, Luca VC, Prentoe J, Hopcraft SE, Blight KJ, Yi M, Lemon SM, Ball JK, Bukh J, Evans MJ, Fremont DH, Diamond MS.** 2011. Neutralizing monoclonal antibodies against hepatitis C virus E2 protein bind discontinuous epitopes and inhibit infection at a postattachment step. J Virol **85:**7005–7019. http://dx.doi.org/10.1128/JVI.00586-11.
32. **Nelson CA, Lee CA, Fremont DH.** 2014. Oxidative refolding from inclusion bodies. Methods Mol Biol **1140:**145–157. http://dx.doi.org/10.1007/978-1-4939-0354-2_11.
33. **Meuleman P, Catanese MT, Verhoye L, Desombere I, Farhoudi A, Jones CT, Sheahan T, Grzyb K, Cortese R, Rice CM, Leroux-Roels G, Nicosia A.** 2012. A human monoclonal antibody targeting scavenger receptor class B type I precludes hepatitis C virus infection and viral spread in vitro and in vivo. Hepatology **55:**364–372. http://dx.doi.org/10.1002/hep.24692.
34. **Hötzel I, Chiang V, Diao J, Pantua H, Maun HR, Kapadia SB.** 2011. Efficient production of antibodies against a mammalian integral membrane protein by phage display. Protein Eng Des Sel **24:**679–689. http://dx.doi.org/10.1093/protein/gzr039.
35. **Mali P, Yang L, Esvelt KM, Aach J, Guell M, DiCarlo JE, Norville JE, Church GM.** 2013. RNA-guided human genome engineering via Cas9. Science **339:**823–826. http://dx.doi.org/10.1126/science.1232033.
36. **Michta ML, Hopcraft SE, Narbus CM, Kratovac Z, Israelow B, Sourisseau M, Evans MJ.** 2010. Species-specific regions of occludin required by hepatitis C virus for cell entry. J Virol **84:**11696–11708. http://dx.doi.org/10.1128/JVI.01555-10.
37. **Grove J, Nielsen S, Zhong J, Bassendine MF, Drummer HE, Balfe P, McKeating JA.** 2008. Identification of a residue in hepatitis C virus E2 glycoprotein that determines scavenger receptor BI and CD81 receptor dependency and sensitivity to neutralizing antibodies. J Virol **82:**12020–12029. http://dx.doi.org/10.1128/JVI.01569-08.
38. **Zhong J, Gastaminza P, Chung J, Stamataki Z, Isogawa M, Cheng G, McKeating JA, Chisari FV.** 2006. Persistent hepatitis C virus infection in vitro: coevolution of virus and host. J Virol **80:**11082–11093. http://dx.doi.org/10.1128/JVI.01307-06.
39. **Dhillon S, Witteveldt J, Gatherer D, Owsianka AM, Zeisel MB, Zahid MN, Rychłowska M, Foung SKH, Baumert TF, Angus AGN, Patel AH.** 2010. Mutations within a conserved region of the hepatitis C virus E2 glycoprotein that influence virus-receptor interactions and sensitivity to neutralizing antibodies. J Virol **84:**5494–5507. http://dx.doi.org/10.1128/JVI.02153-09.
40. **Tao W, Xu C, Ding Q, Li R, Xiang Y, Chung J, Zhong J.** 2009. A single point mutation in E2 enhances hepatitis C virus infectivity and alters lipoprotein association of viral particles. Virology **395:**67–76. http://dx.doi.org/10.1016/j.virol.2009.09.006.
41. **Kim CS, Keum SJ, Jang SK.** 2011. Generation of a cell culture-adapted hepatitis C virus with longer half life at physiological temperature. PLoS One **6:**e22808. http://dx.doi.org/10.1371/journal.pone.0022808.
42. **Kaul A, Woerz I, Meuleman P, Leroux-Roels G, Bartenschlager R.** 2007. Cell culture adaptation of hepatitis C virus and in vivo viability of an adapted variant. J Virol **81:**13168–13179. http://dx.doi.org/10.1128/JVI.01362-07.

43. **Russell RS, Meunier J-C, Takikawa S, Faulk K, Engle RE, Bukh J, Purcell RH, Emerson SU.** 2008. Advantages of a single-cycle production assay to study cell culture-adaptive mutations of hepatitis C virus. Proc Natl Acad Sci U S A **105:**4370–4375. http://dx.doi.org/10.1073/pnas.0800422105.
44. **Sabahi A, Uprichard SL, Wimley WC, Dash S, Garry RF.** 2014. Unexpected structural features of the hepatitis C virus envelope protein 2 ectodomain. J Virol **88:**10280–10288. http://dx.doi.org/10.1128/JVI.00874-14.
45. **Song H, Ren F, Li J, Shi S, Yan L, Gao F, Li K, Zhuang H.** 2012. A laboratory-adapted HCV JFH-1 strain is sensitive to neutralization and can gradually escape under the selection pressure of neutralizing human plasma. Virus Res **169:**154–161. http://dx.doi.org/10.1016/j.virusres.2012.07.022.
46. **Bungyoku Y, Shoji I, Makine T, Adachi T, Hayashida K, Nagano-Fujii M, Ide Y-H, Deng L, Hotta H.** 2009. Efficient production of infectious hepatitis C virus with adaptive mutations in cultured hepatoma cells. J Gen Virol **90:**1681–1691. http://dx.doi.org/10.1099/vir.0.010983-0.
47. **Kang J-I, Kim JP, Wakita T, Ahn B-Y.** 2009. Cell culture-adaptive mutations in the NS5B gene of hepatitis C virus with delayed replication and reduced cytotoxicity. Virus Res **144:**107–116. http://dx.doi.org/10.1016/j.virusres.2009.04.002.
48. **Pokrovskii MV, Bush CO, Beran RKF, Robinson MF, Cheng G, Tirunagari N, Fenaux M, Greenstein AE, Zhong W, Delaney WE, Paulson MS.** 2011. Novel mutations in a tissue culture-adapted hepatitis C virus strain improve infectious-virus stability and markedly enhance infection kinetics. J Virol **85:**3978–3985. http://dx.doi.org/10.1128/JVI.01760-10.
49. **Liu S, Xiao L, Nelson C, Hagedorn CH, Hagedorn C.** 2012. A cell culture adapted HCV JFH1 variant that increases viral titers and permits the production of high titer infectious chimeric reporter viruses. PLoS One **7:**e44965. http://dx.doi.org/10.1371/journal.pone.0044965.
50. **Aligeti M, Roder A, Horner SM.** 2015. Cooperation between the hepatitis C virus p7 and NS5B proteins enhances virion infectivity. J Virol **89:**11523–11533. http://dx.doi.org/10.1128/JVI.01185-15.
51. **Pileri P, Uematsu Y, Campagnoli S, Galli G.** 1998. Binding of hepatitis C virus to CD81. Science **282:**938–941. http://dx.doi.org/10.1126/science.282.5390.938.
52. **Law M, Maruyama T, Lewis J, Giang E, Tarr AW, Stamataki Z, Gastaminza P, Chisari FV, Jones IM, Fox RI, Ball JK, McKeating JA, Kneteman NM, Burton DR.** 2008. Broadly neutralizing antibodies protect against hepatitis C virus quasispecies challenge. Nat Med **14:**25–27. http://dx.doi.org/10.1038/nm1698.
53. **Barth H, Schafer C, Adah MI, Zhang F, Linhardt RJ, Toyoda H, Kinoshita-Toyoda A, Toida T, Van Kuppevelt TH, Depla E, Von Weizsacker F, Blum HE, Baumert TF.** 2003. Cellular binding of hepatitis C virus envelope glycoprotein E2 requires cell surface heparan sulfate. J Biol Chem **278:**41003–41012. http://dx.doi.org/10.1074/jbc.M302267200.
54. **Germi R, Crance J-M, Garin D, Guimet J, Lortat-Jacob H, Ruigrok RWH, Zarski J-P, Drouet E.** 2002. Cellular glycosaminoglycans and low density lipoprotein receptor are involved in hepatitis C virus adsorption. J Med Virol **68:**206–215. http://dx.doi.org/10.1002/jmv.10196.
55. **Monazahian M, Böhme I, Bonk S, Koch A, Scholz C, Grethe S, Thomssen R.** 1999. Low density lipoprotein receptor as a candidate receptor for hepatitis C virus. J Med Virol **57:**223–229. http://dx.doi.org/10.1002/(SICI)1096-9071(199903)57:3<223::AID-JMV2>3.0.CO;2-4.
56. **Agnello V, Abel G, Elfahal M, Knight GB, Zhang QX.** 1999. Hepatitis C virus and other flaviviridae viruses enter cells via low density lipoprotein receptor. Proc Natl Acad Sci U S A **96:**12766–12771. http://dx.doi.org/10.1073/pnas.96.22.12766.
57. **Bartosch B, Vitelli A, Granier C, Goujon C, Dubuisson J, Pascale S, Scarselli E, Cortese R, Nicosia A, Cosset F-L.** 2003. Cell entry of hepatitis C virus requires a set of co-receptors that include the CD81 tetraspanin and the SR-B1 scavenger receptor. J Biol Chem **278:**41624–41630. http://dx.doi.org/10.1074/jbc.M305289200.
58. **Flint M, Maidens C, Loomis-Price LD, Shotton C, Dubuisson J, Monk P, Higginbottom A, Levy S, McKeating JA.** 1999. Characterization of hepatitis C virus E2 glycoprotein interaction with a putative cellular receptor, CD81. J Virol **73:**6235–6244.
59. **Evans MJ, von Hahn T, Tscherne DM, Syder AJ, Panis M, Wölk B, Hatziioannou T, McKeating JA, Bieniasz PD, Rice CM.** 2007. Claudin-1 is a hepatitis C virus co-receptor required for a late step in entry. Nature **446:**801–805. http://dx.doi.org/10.1038/nature05654.
60. **Ploss A, Evans MJ, Gaysinskaya VA, Panis M, You H, de Jong YP, Rice CM.** 2009. Human occludin is a hepatitis C virus entry factor required for infection of mouse cells. Nature **457:**882–886. http://dx.doi.org/10.1038/nature07684.
61. **Hopcraft SE, Evans MJ.** 2015. Selection of a hepatitis C virus with altered entry factor requirements reveals a genetic interaction between the E1 glycoprotein and claudins. Hepatology **62**(4):1059–1069. http://dx.doi.org/10.1002/hep.27815.
62. **Dao Thi VL, Granier C, Zeisel MB, Guérin M, Mancip J, Granio O, Penin F, Lavillette D, Bartenschlager R, Baumert TF, Cosset F-L, Dreux M.** 2012. Characterization of hepatitis C virus particle subpopulations reveals multiple usage of the scavenger receptor BI for entry steps. J Biol Chem **287:**31242–31257. http://dx.doi.org/10.1074/jbc.M112.365924.